Technical Foundation Memo 1

To: Susannah Howe

From: VAWT Ventures

Date: October 17, 2025

Subject: A technical overview of theoretical VAWTs, HAWTs vs VAWTs, and Design Review 1 feedback question/answers

Introduction

This memo aims to give a sufficient technical foundation on vertical axis wind turbines (VAWTs) for the ideation phase to start successfully. This memo will cover an overview and detailed comparison between HAWTs and VAWTs, provide a technical foundation of Savonius and Darrieus type VAWTs, and give an overview of the structural mechanics associated with wind turbines.

Table of Contents:

HAWT vs VAWT

Horizontal axis wind turbines (HAWTs) and vertical axis wind turbines (VAWTs) are two broad categories of wind turbine. VAWTs have an axis of rotation perpendicular to the direction of the wind. These differ from HAWTs, which have an axis of rotation parallel to the wind. HAWTs and VAWTs have different benefits, drawbacks, and applications, which will be discussed in this section.

HAWTs are typically used in large wind farm applications in remote and offshore locations with access to clean and undisturbed air [1]. HAWTs function well when their rotors are facing the wind flow, so they are usually equipped with a self-starter and a yaw system which turns the blade towards the wind [1][2]. Their ideal aerodynamic efficiency is reported within the range of 40-55% under steady wind, however, their performance diminishes sharply in low or unsteady wind conditions. Most commercial wind turbines are HAWTs due to their high efficiencies and overall better performance [1].

In 2023, wind power made up about 10.2% of total U.S. electricity generation [9]. Nearly all of this comes from horizontal-axis wind turbines (HAWTs), with vertical-axis wind turbines (VAWTs) contributing under 1% of total generation.

In contrast, VAWTs are a much less developed technology. Although they are less prominent, they have many advantages over HAWTs depending on the application. A key benefit is their multidirectional nature, allowing them to take advantage of wind in multiple directions without a direction control mechanism. This allows them to function better in the turbulent wind conditions found in urban areas. In addition, they tend to be simpler, lower cost in both construction and maintenance, and they have lower noise emissions and vibrations due to their slower rotational speeds [3]. However, they struggle with low efficiencies and low market penetration.

In recent years, the trend in wind power has been to increase the size of the turbines. For off-shore applications, this is especially important because foundation and installation costs are so high that it is more economical with larger, higher power output turbines. HAWTs have become so economical that VAWTs may not be able to beat them for large scale applications.

However, small VAWTs can play a role in areas where HAWTs are not effective, such as within urban environments [1].

The following table summarizes these key differences between HAWTs and VAWTs:

Table 1 : Benefits, drawbacks, and applications of VAWTs and HAWTs

	VAWT	HAWT
Benefits	• Smaller [10] • Lower noise [4] • Lower vibration [4] • Better performance with changing wind directions and turbulence [2][3] • cheaper/easier maintenance [5] • Lower upfront costs [5]	• 40-55% efficiency under steady wind [7] • Better all around performance [7] • Proven technology widely used in wind farms [2] • Wide range of commercial product options [2] • Cost effective [5]
Drawbacks	• Less efficient [7] • Not well proven [2] • Lower market penetration	• Performs poorly with changing wind directions [2] • Higher noise and vibration [4] • Larger [10]
Applications	• Urban environments [7] • Distributed energy [7] • Smaller scale [7]	• Medium to large scale • centralized/grid level energy • Flat terrain wind conditions [3]

3

What are the causes of urban airflow conditions that are tricky for HAWTs? Why are VAWTs better?

There are many challenges associated with urban airflow conditions for both HAWTs and VAWTs. Urban areas include structures that increase the surface roughness when compared with flat terrain, impacting the velocity field as shown in Figure 1 [2][3]. The increased surface roughness causes the average wind speeds to be lower in urban areas [2]. The power that can be extracted from the wind increases with the cube of wind velocity as shown in Equation 1 [2]:

$$P_{wind} = \frac{1}{2}\rho A U^3 \quad (1)$$

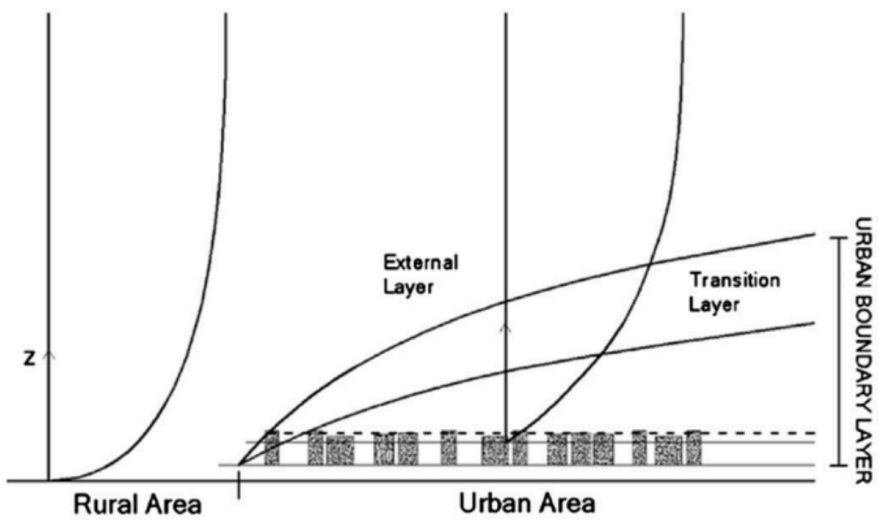

Figure 1: 4. Urban boundary layer and velocity profile in urban environments (right) and flat terrain (left) [3]

However, as air is forced around buildings, trains, and structures, regions with higher local average velocities and increased density are created. This obstruction of the flow path also causes rapid changes in flow direction and higher levels of turbulence intensity [2][3]. Turbulence intensity measures turbulence strength and is defined as the standard deviation of the horizontal wind speed divided by the mean wind speed over a time period [71]. High turbulence intensity signifies large fluctuations in wind speed, which puts extra loads on wind turbines [3]. The slower average wind speeds combined with turbulent flow characterized by rapid changes in

wind direction and velocity pose challenges for the design of efficient and effective wind turbines [2].

HAWTs are designed to operate well in open areas with consistent wind conditions. To function well, their rotors need to be facing the wind flow. While they do have yaw systems that allow the turbine to rotate to face the wind, the constant change in directions of air in urban areas exceeds this ability. Because of this, HAWTs have lower performance in the turbulent wind conditions found in urban areas [2].

VAWTs perform better in these areas due to their omnidirectional nature which allows them to take advantage of winds with changing flow directions [2]. In addition, their lower “cut in” wind speed allows them to take advantage of the slower winds as well [1].

In a simulation of airflow around a symmetric flat-roofed building with length much greater than its height performed by Toja-Silva et.al, it was found that in an urban environment, the multidirectional character of the wind plays a more important role than the incident velocity. Various wind turbines were then superimposed on the resulting velocity fields using a wind speed of 1m/s. The results of this qualitative analysis show that for HAWTs, the multidirectional wind conditions are incompatible with normal turbine operation and subject the HAWT to loads beyond its design specifications. In contrast, when a generic VAWT (valid for Darrieus, Giromill, or Savonius) was superposed over the same airflow conditions, the conditions were shown to be compatible with wind turbine operation [3]. This demonstrates that while HAWTs perform better in open, flat-terrain environments, VAWTs are superior for high-density building environments with turbulent airflow conditions [3].

Who are potential users for VAWTs? What locations are best suited?

Some potential beneficiaries of the advancement of VAWT technology are residential buildings [11][12], commercial and industrial buildings [13][14], single-family homes [15], on top of utility poles [16], highrise buildings [17][18], offshore and onshore wind farms [19], and campuses going carbon neutral [20]. There are many different users and locations our VAWT could be designed towards, however we chose to focus on campuses going carbon neutral. Smith

is an easily accessible campus with the goal of going Carbon Neutral by 2030, so we will be designing a VAWT for a Smith building. Though targeted towards colleges, our VAWT has the potential to provide insight for the technology in any urban to semi-urban location. This research could be applied to residential buildings, commercial and industrial buildings, or single-family homes in areas with turbulent wind conditions.

How much do VAWTs minimize noise and vibration compared to HAWTs?

VAWTs minimize both noise and vibration as compared to HAWTs on a similar scale. When comparing noise levels, it is important to understand what sound is. Sound is a pressure wave that travels through a medium [21], and it can be divided into two types of measurements. Sound emission is the sound power level and it is defined by Equation 1, as the rate of sound production energy of a given source:

$$L_W = 10 \cdot log_{10}(\frac{P}{P_o}) \quad [1]$$

where P_o is a reference power level given of 10^{-12} Watts and P is the pressure in the sound wave in Pascals. As seen in Equation 1, the sound power level is the total acoustic energy emitted by the given source, and it is measured in decibels, relative to the given reference power. Decibels are a unit of measurement for the intensity or amplitude of sound. Since the Decibel is on a logarithmic scale, each 10 decibel increase means a tenfold increase in the sound power. For reference, human hearing ranges from around 65 dB (the sound of a speaking voice) to 150 dB (the sound of fireworks or jet engines) [22].

The other way to measure sound is the sound pressure level, or noise immission. The sound pressure level measures the pressure fluctuations caused by sound waves to quantify “loudness.” Sound pressure levels are also measured on a logarithmic scale, and use a reference level p_o of 20 μPa for air. Since the sound pressure level is a measurement at a specific point, this measurement depends on the distance from the source and the environment, or in other words, this measurement will decrease with distance.

$$L_p = 10 \cdot log_{10}(\frac{p^2}{p_o^2}) \quad [2]$$

Sound pressure levels and sound power levels differ in that one varies with distance and environment while the other is a constant property of the source, respectively. Sound power levels are useful in comparing different sources, while sound pressure is useful for knowing the sound levels at a certain location given by one source.

Currently, the legal noise limit for current horizontal axis wind turbines is 40 to 45 dB(A) at a distance of 300m, because most wind farms are kept at a minimum of 300m away from people who would be hearing the noise [28]. Legal sound levels for VAWTs are regulated state by state, and for Massachusetts specifically, this is regulated by the Department of Environmental Protection (MassDEP) noise policy and local municipal bylaws. The MassDEP performed the Kingston Wind Independence (KWI) Turbine Acoustical Monitoring Study in April 16, 2015 to determine the sound regulations for the state, and this was conducted in response to requests from KWI and the Kingston Board of Health to the Massachusetts Clean Energy Center (MassCEC) and Massachusetts Department of Environmental Protection (MassDEP). From the study, MassDEP concluded that sound emissions cannot exceed 10 dBA above the ambient sound level at the nearest property line. This applies to all new noise sources, including vertical axis wind turbines [29].

Noise emitted from wind turbines can also be divided into mechanical and aerodynamic noise. The mechanical noise comes from the gearbox and the mechanics of the system while the aerodynamic noise is due to the wind force on the blades, and the movement of the blades through the fluid (air). For HAWTs most of the aerodynamic noise is generated by the wing tip as the blade travels down, which relates to moving airfoil [23]. Due to lower tip speed ratio, as compared to HAWTs, the blade velocity that generates aerodynamic noise is comparatively lower for VAWTs. In a study performed by Möllerström, E., Ottermo, F., Hylander, J., and Bernhoff, H, numerical methods were used to simulate aerodynamic noise from VAWTs. The study was performed and then compared to a similar scale HAWT. The results are shown in the two figures below, showing that the VAWTs have lower dB than the HAWTs at the same wind speeds. [24]

Table 2. Noise emission for different wind speeds calculated from results of recordings.

Wind Speed at 10 m Height	Tip Speed Ratios (TSR)	Noise Emission with Standard Uncertainty	Noise Model Calculation
m/s	-	dBA	dBA
5	3.8	93.1 ± 1.0	69.6
6	3.8	94.1 ± 1.1	74.5
7	3.4	95.4 ± 1.0	78.6
8	2.9	96.2 ± 1.0	82.3

(a)

Table 3. Noise emission and specifications of horizontal axis wind turbines (HAWTs) in comparison. Wind speeds for noise emissions are stated for 10 m above ground [27,28,29,30].

Turbine Model	Power (kW)	Rotor Diameter (m)	No. of Blades	Power Regulation	dBA at 6 m/s	dBA at 8 m/s
Vestas V27	225	27	3	Pitch	96.7	97.3
GEV-MP R	200–275	32	2	Pitch	100.2	102.4
WTN250	250	30	3	Stall	95.1	99.8
Norwin 29/225	225	29	3	Stall	95.2	97.5

(b)

Figure 2: Möllerström, E., Ottermo, F., Hylander, J., and Bernhoff, H Study showing Noise Models in dBA for a T1-turbine (VAWT) and a similar scaled HAWT

The T1-turbine (VAWT) indicates a noise emission at the absolute lower range of the similar size HAWTs while running at optimum tip speed. At 8 m/s, for example, the noise emission of the T1-turbine was 96.2 ± 1.0 dBA which is significantly lower than the range of measurements for the HAWTs of 97.3 dBA - 102.4 dBA [24].

In another study, performed in Sweden, called the Noise Propagation from a Vertical Axis Wind Turbine [25], initial noise measurements were performed on a 200kW vertical axis wind

turbine (VAWT) and results were compared to that of a Vestas V27, a similar size horizontal axis wind turbine (HAWT). The results from the propagation measurements indicated that noise declines more rapidly with distance for the VAWT than for the reference HAWT.

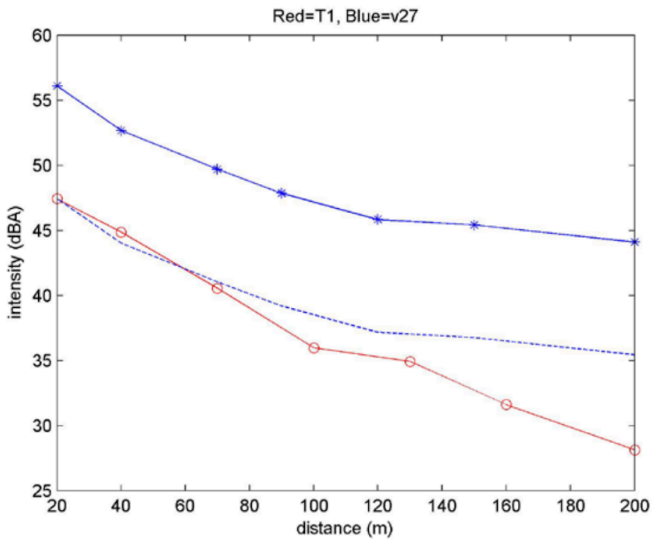

Figure 7: Noise propagation between T1 (red °) and V27 (blue *) turbines. Dashed blue line is the blue line projected for comparison

Figure [3] Noise Propagation comparing a VAWT to a similar scaled HAWT

As seen above in Figure 3, the noise propagation declines at a more steep rate for the red line (VAWT), but also the initial recording at a distance of 20 m is lower for the VAWT, at about 47 dBA than for the HAWT at about 56 dBA.

9

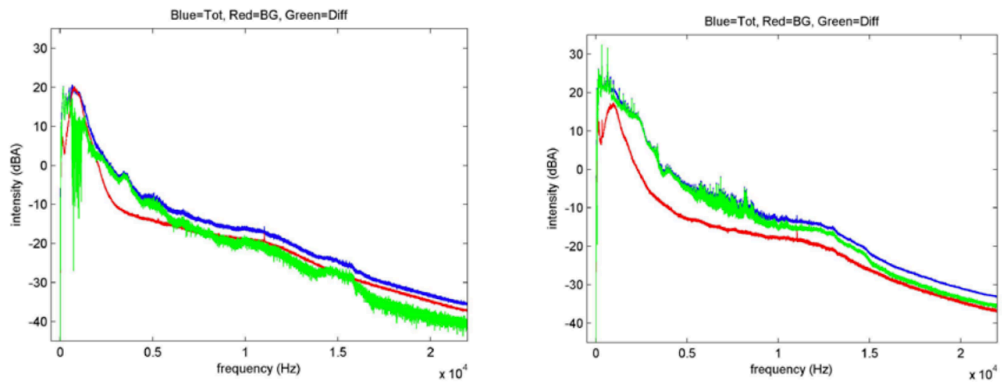

Figure 4: Frequency distribution for T1 (left) and V27 (right). Total noise in blue (highest for high frequencies), background noise in red (in middle for high frequencies) and difference between total and background noise in green (lowest for high frequencies).

Figure [4] ERIK MÖLLERSTRÖM, SEBASTIAN LARSSON, FREDERIC OTTERMO, JONNY HYLANDER, and LARS BÅÅTH, frequency distribution for the T1 (VAWT) on the left, and V27 (HAWT) on the right

In the frequency distribution plot, it is also evident that for the VAWT, the intensity remains lower at all frequencies as compared to the similarly scaled HAWT measured under the same constants and constraints. From both of these studies, it can be concluded that VAWTs produce less noise and vibration as compared to HAWTs, and these levels can be further minimized through the optimization phase, where we will test and simulate to design a VAWT that produces the least amount of noise pollution.

How does the cost and noise of VAWTs compare to HAWTs at a similar scale?

VAWTs are not generally cheaper to manufacture and install than HAWTs when compared on a similar scale for commercial-scale power generation. Additionally, VAWTs energy conversion efficiency is generally lower. This means that, over time, the cost per unit of electricity generated is typically higher for VAWTs: estimates place VAWT power generation costs at around 20-30% higher than HAWTs on comparable scales [30].

In addition, when comparing the manufacturing costs of VAWTs and HAWTs, it must be considered that HAWTs have been produced for much longer than VAWTs and are produced in large numbers. The longer history of HAWT production gives rise to smarter and cheaper solutions and the large numbers decrease the price since parts can be mass produced. Finally, as HAWT technology has matured, their scale could be increased, lowering the cost per installed kW further. There has not been mass production of VAWTs [32]

In a recent study performed by Ahmad Shah Irshad, the Multi Objective Genetic Algorithm (MOGA) in MATLAB software was used for the sizing of hybrid sustainable energy systems with wind turbines (HAWTs and VAWTs) [26]. In Figure 5 shown below, the cost of energy, net present cost, and total cost for the HAWT was calculated to be 0.02 $/kWh, $85,905, and $332,240, respectively. For a similarly scaled VAWT, these values were 0.06 $/kWh, $129,932, and $502,511 respectively.

Table 3. Comparative result of the two cases.

Parameters	HAWT	VAWT
Total energy (kWh/year)	487,497	391,063
Total renewable energy (kWh/year)	392,541	208,015
Renewable fraction (%)	80.5	53.2
CO_2 emissions (kg/year)	78,813	151,929
Saving in CO2 (kg/year)	325,809	172,652
Share of PV (%)	11	37
Share of wind (%)	70	17
Share of grid (%)	19	47
NPC ($)	85,905	129,932
Total cost of the system ($)	332,240	502,511
COE ($/kWh)	0.02	0.06
Amount of PV (kW)	31.5	87.7
Amount of wind (kW)	61.6	26.2

Figure [5] Economic comparative analysis performed on a VAWT vs HAWT

In another recent study (2024) by Rosato et.al, a techno-economic evaluation was conducted for three different scaled VAWTs and then compared to similarly scaled HAWTs [27]. These were: Pico (<100 Watts), Micro (50-1000 Watts), and Mini VAWT (1000 - 1500 Watts).

Table 8. Main characteristics of commercially available vertical axis Mini wind turbines (VAMNWTs).

Savonius-Darrieus-Hybrid/Manufacturer/Model/Number of Blades	Start-Up/Cut-In/Cut-Out/Survival Wind Speed (m/s)	Maximum Power (W)/Voltage (V)	Rotor Diameter/Turbine Length/Tower Height (m)	Capital Cost (EUR)/Specific Capital Cost (EUR/W)	Materials of Blades	Noise Level	Battery Capacity (Ah)
Darrieus/SISHUINIANHUA/Ruxmy/5 [241]	2.0/NA/NA/45.0	NA/12–24 (NA)	0.90/0.6/NA	568.05/NA	Nylon fibre	NA	NA
Savonius/NA/Wangyongqi/2 [242]	1.5/3.0/NA/40.0	9100/12–220 (AC)	0.47/1.08/7.0–12.0	274.77/0.03	Resin Glass and Basalt	NA	NA
Darrieus/SMJY/SMJY/3 [243]	1.3/2.3/NA/40.0	NA/12–220 (NA)	0.6/0.75/7.0–12.0	2051.0/NA	Fibreglass	NA	NA
Darrieus/Hipar sp.z.o.o./ECOROTE 9800/4 [244]	1.2/3.0/25.5/NA	12,000/230 (AC)	4.3/5.6/9.0	28,588.40/2.38	Aluminium	46 dB at 8.0 m/s	NA
Hybrid/FlexPro/EOL-V/5 External Darrieus + 4 Internal Savonius [245]	3.0/NA/NA/50.0	12,000/380 (NA)	4.5/NA/12.0	21,800.0/1.82	Glass Fibre Reinforced Polymer	NA	NA
Darrieus/Ecolibri Srl/EW01/3 [246]	3.5/5.0/15.0/NA	14,000/380 (NA)	5.7/6.0/10.0	10,000.0/0.71	Composite	NA	NA
Darrieus/AEOLOS/Aeolos-V10/3 [247,248]	1.5/2.5/40.0/52.5	12,000/300–380 (NA)	4.5/4.8/NA	19,057.97/1.59	Aluminium	45 dB	NA
Darrieus/SunSurfs/WT3-10/3 [249]	1.8/NA/8.0/28.0	10,700/360–400 (AC)	9.0/NA/12.0	27,335.54/2.56	NA	63 dB	NA
Darrieus/SunSurfs/WT3-20/3 [250]	1.8/NA/9.0/28.0	21,400/360–400 (AC)	11.0/12.0/12.0	59,600.22/2.79	NA	63 dB	NA
Darrieus/SunSurfs/WT3-30/3 [251]	1.8/2.9/9.0/28.0	32,100/400 (AC)	12.0/12.0/12.0	87,108.01/2.71	NA	65 dB at 5.0 m/s with 10 m distance	NA
Savonius/WINDSIDE/WS-12/2 [252,253,254]	2.0/2.5/40.0/60.0	25,000/12–48 (DC)	2.0/8.0/10	NA/NA	Aluminium	2–5 dB with 2 m distance	NA
Savonius/TESUP/Hera Wind Pro/2 [104,255]	1.0/2.0/15.0/50.0	7032/220 (NA)	0.40/1.12/NA	1380.0/0.20	Aluminium	35 dB	NA
Savonius/TESUP/Atlas 7/2 [104,256]	1.5/2.0/17.0/50.0	7032/220 (NA)	1.20/1.126/NA	1460.0/0.21	Aluminium	30 dB	NA
Savonius/TESUP/Atlas X7/3–12 [104,257]	1.0/2.0/19.0/50.0	7032/220 (NA)	0.46/1.126/NA	1380.0/0.20	Aluminium	30 dB	NA

Table 7. Main characteristics of commercially available horizontal axis mini wind turbines (HAMNWTs).

Manufacturer/Model/Number of Blades	Start-Up/Cut-In/Cut-Out/Survival Wind Speed (m/s)	Maximum Power (W)/Voltage (V)	Rotor Diameter/Turbine Length/Tower Height (m)	Capital Cost (EUR)/Specific Capital Cost (EUR/W)	Materials of Blades	Noise Level	Battery Capacity (Ah)
Qingdao Anhua New Energy Equipment Co./Horizontal Axis Wind Turbine with Maglev Generator/3 [232]	2.5/3.0/30.0/60.0	11,000/240–500 (AC)	7.6/NA/12.0	NA/NA	Fibreglass reinforced	65 dB	NA
Bergey Windpower/Excel 10/3 [233,234]	2.24/3.4/59.9/59.9	12,600/220–240 (AC)	7.01/NA/18.0–49.0	29,770.08/2.36	NA	42.9 dB	NA
Bergey Windpower/Excel 15/3 [234,235]	3.13/4.47/59.9/59.9	21,800/230–240 (AC)	9.6/5.21/18.0–49.0	35,139.38/1.60	Carbon fibre	48.5 dB	NA
Ryse Energy/E-10/3 [236,237]	NA/2.0/30.0/70.0	20,000/NA	9.8/NA/15.0–36.0	69,707.41/3.49	Fibreglass	33, 40, 46 dB at 180, 100, 46 m distances	NA
GEATECNO/Gaia-Wind 133-11kW/2 [238,239]	2.5/3.5/10.0/25.0	12,000/400 (NA)	13.0/NA/NA	35,946.90/3.00	NA	20, 40, 60 dB at 100, 60, 30 m distances	NA
InkPV or OEM/FD-30000/3 [240]	3.0/NA/30.0/60.0	33,000/220–380 (DC)	12.0/NA/NA	43,775.18/1.33	Fibreglass	55 dB	NA

Figure [6] Characteristics of commercially available VAWTs (Table 6.) and HAWTs (Table 7.)

These values show that for the Pico and Micro VAWTs, the average specific capital costs are 6.24 EUR/W and 4.18 EUR/W, respectively. While for Pico and Micro HAWTs those values are 3.72 EUR/W and 1.38 EUR/W, respectively. Therefore, the average capital costs are lower for the scaled HAWTs for pico and micro turbines. However, for the mini VAWTs, the average specific capital cost was 1.38 EUR/W, and 2.36 EUR/W for the HAWT. So, for mini wind turbines, VAWTs turn out to be the cheaper option.

Do VAWTs pose less risk to wildlife than HAWTs?

Currently, there is no empirical evidence to support the claim that vertical-axis wind turbines (VAWTs) pose less risk to wildlife than horizontal-axis wind turbines (HAWTs). A review of small urban wind turbines (SUWT), which includes both VAWTs and HAWTs, found that while urban wildlife may be affected, only two studies in the article even mention wildlife impacts, and neither provide field data [33]. Most existing work focuses on public perception or theoretical risks rather than measured outcomes. In another study focused on the correlation between energy production and wildlife fatalities, it was found that avian and bat mortality rate was constant per unit of energy produced across all sizes and types of turbines [34].

Darrieus Wind Turbine

Darrieus type turbines are one of two main vertical axis wind turbine types, designed in the year 1931 by Georges Darrieus, a French aeronautical engineer. Darrieus wind turbines are also known as the Egg Beater turbine [35]. Darrieus wind turbines are lift based meaning that they generate energy from the wind by generating lift. Lift is a force acting perpendicular to the direction of an object's motion through a fluid. The drawbacks of Darrieus type turbines are their relatively low starting torque which means an external source must start the turbine up.

Figure 6. Darrieus Vertical Axis Wind Turbine on top of a home

Benefits

Darrieus Wind turbines have high efficiency as compared to drag based types. This is mainly due to its aerodynamic efficiency from the lift-based mechanism. This mechanism allows the turbine to achieve very high rotational speeds, by utilizing the lift force, similar to how airplane wings function [45]. Compared to the drag types, Darrieus types are more effective at generating electricity at higher wind speeds, and have more consistent energy output. Darrieus wind turbines are also omnidirectional, meaning that the rotor can receive wind from any direction. This is something that horizontal wind turbines are not capable of, and why VAWTs are a great innovation for the multidirectional wind conditions of urban areas. Darrieus vertical axis wind turbine achieves 30% to 40% overall efficiency rate [35]. Due to their consistent and smooth energy output, they are also useful in situations that require consistent energy output, like larger scale applications [39].

Shortcomings/Modes of Failure

Darrieus wind turbines have a very low starting torque, so it is very difficult to start it and it usually requires an external energy source. In current research, designers have tried to optimize the low initial torque by creating hybrids of the Savonius type and Darrieus (incorporating the self-starting mechanism of the Savonius turbine) [47]. Additionally, current researchers have used mechanical systems to optimize the blade pitch and have studied the specific blade profiles that are capable of making the Darrieus self-starting [48] [49]. In another study, performed by M. Douak and Z. Aouachria, variable pitch machines were tested to see if this would optimize the low initial torque of a Darrieus turbine with NACA-0015 airfoil blades. Variable pitch machines have blades that can be rotated about their axis, which changes the blades' pitch angle. This, in turn, alters the angle of attack and increases torque [46]. In Figure 2 shown below, the optimized design is shown where the blades are allowed to rotate about an axis along its pitch, where the angle of attack (α) is the acute angle between the wind and the chord line of the airfoil, U is the blade speed and V is the wind speed at the rotor.

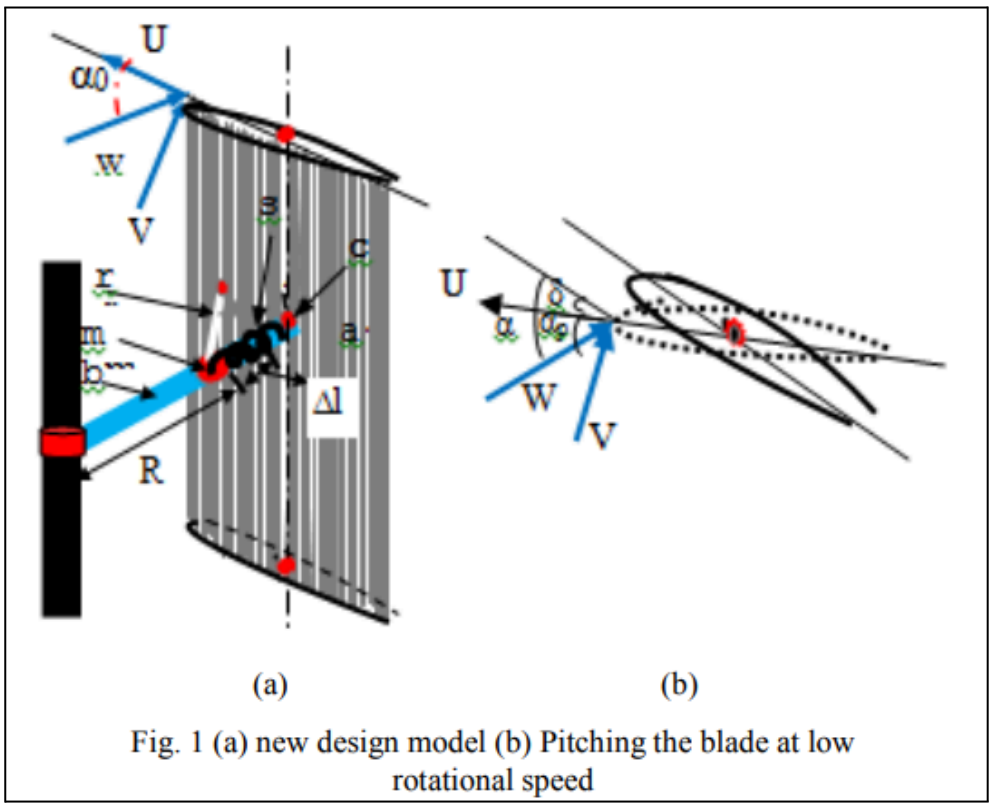

Fig. 1 (a) new design model (b) Pitching the blade at low rotational speed

Figure 7. Darrieus Design by M. Douak and Z. Aouachria

It is necessary to know that for any airfoil to generate lift, the attack angle must remain less than the airfoil stalling angle [46]. The stalling angle of the airfoil is determined from the lift coefficient curve of the airfoil. Furthermore, it was found by this study that the optimal tip speed ratio λ =U/V was in the range (4°-10°). Here the attack angle remains smaller than the stalling angle and so lift is produced for this range.

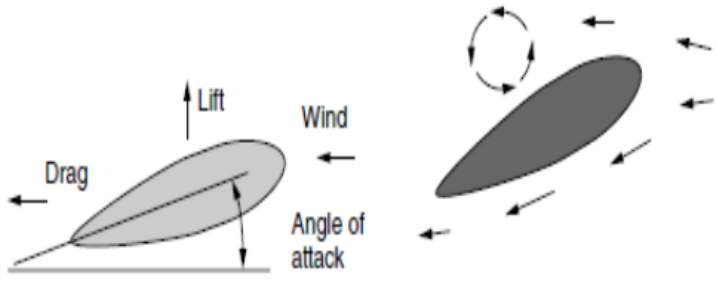

(a) Angle of attack (b) Stall case

16

Figure 8. Diagram of Angle of Attack and Stall Case measurements

Aerodynamics:

Darrieus wind turbines typically consist of two vertically oriented blades that rotate about a perpendicular central shaft. Operation begins when a small auxiliary motor initiates the rotation of the rotor. As the rotational speed increases, airflow over the blade surfaces generates aerodynamic torque. This aerodynamic force sustains and enhances rotation in the direction of the prevailing wind flow, allowing the device to operate efficiently once self-sustained motion is achieved. Lift is created by pressure differences on either side of the blade, which are caused by the airflow around the airfoil. As wind moves more quickly over the curved, longer upper surface of the blade, the pressure above decreases. Meanwhile, slower airflow along the lower, flatter surface produces higher pressure beneath the blade. The resulting pressure imbalance generates a lifting force that acts perpendicular to the wind direction [35] [44].

Parameters:

The rotor assembly comprises multiple curved aerofoil blades attached to the primary rotary shaft.

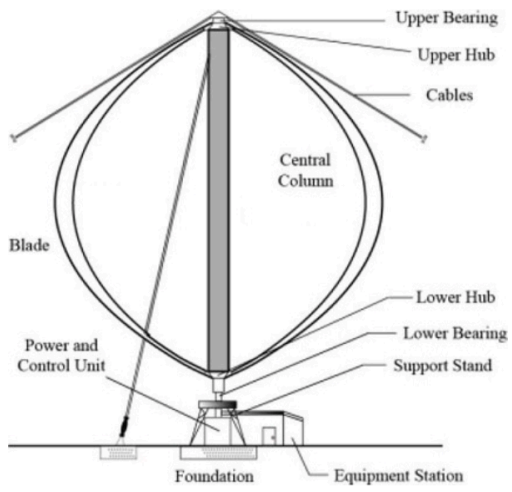

Figure 9. Darrieus Wind Turbine Design Components

Most modern configurations employ symmetrical NACA airfoil profiles, with thickness ratios ranging from 12% to 21%, optimized for stable aerodynamic performance and reduced drag. These airfoils, such as the NACA 0012 profile, are commonly used due to their well-documented aerodynamic characteristics and predictable behavior under varying flow conditions [40].

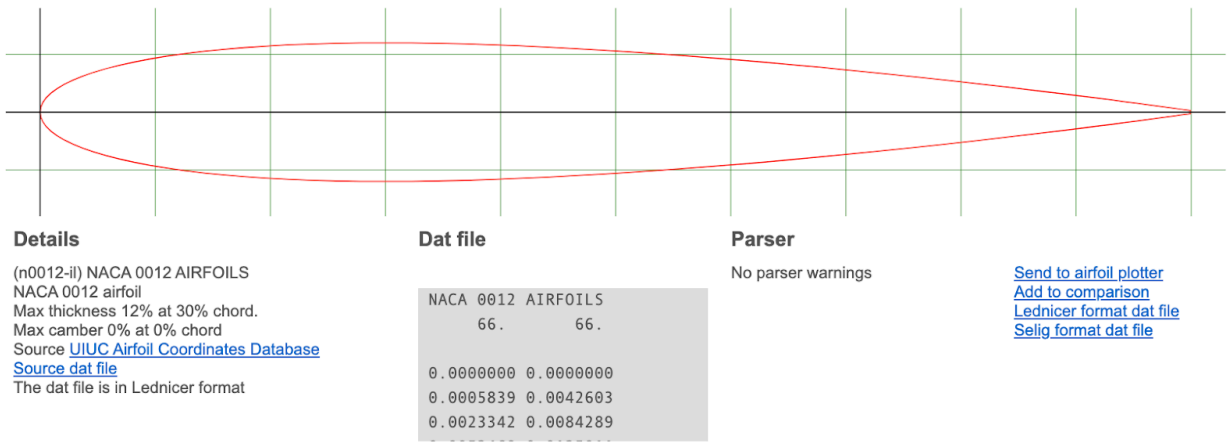

Figure 10. NACA 0012 AIRFOILS (n0012-il), taken from AirFoil Tools

Calculations

When calculating the power or efficiency of a Darrieus wind turbine, estimable parameters can be used. The first is accessible wind power, modeled by equation 1:

$$P_{wind} = \frac{1}{2}\rho v^3 A \qquad [1]$$

Equation 1 expresses the kinetic power available in the wind passing through the rotor area, where ρ is the density of air in kg/m^3, v is the velocity of the wind in m/s, A is the rotor swept area, and P is the total kinetic power in the wind (W). Another parameter is the wind turbine efficiency which is modeled by equation 2 below:

$$\mu = (1 - k)(1 - k_e)(1 - k_{e,t})(1 - k_t)(1 - k_w)C \qquad [2]$$

Where μ is the overall (real) efficiency of the system, k is the miscellaneous mechanical and aerodynamic losses, k_e is the electrical losses within the turbine (e.g., generator inefficiency,

internal resistance), $k_{e,t}$ is the electrical transmission losses between turbine and grid, k_t is the fractional time lost due to operational downtime/maintenance, k_w is the wake losses where, a wake is a cylinder of air downwind of a turbine in which the wind speed is reduced because of the wind energy that has been extracted by the turbine. The loss of energy generation capacity of the downstream turbines due to this wake effect is collectively referred to as wake losses [37], and C is the correction coefficient for secondary losses. Each (1−k) term represents the efficiency retained after a specific category of loss. Multiplying them all gives the total efficiency of the turbine system from wind input to electrical output. The coefficient of power C_P for a lift-based wind turbine can be expressed in terms of the tip speed ratio, the coefficient of lift, and the coefficient of drag [16]. A derived formula that incorporates these quantities is:

$$C_P = C_L\sqrt{1 + \lambda^2}(\lambda - \gamma\lambda^2) \quad [3]$$

Where λ is the Tip Speed Ratio defined below in equation 6, and γ is the ratio of the coefficient of drag to the coefficient of lift (C_D/C_L). Another key parameter for calculations regarding the Darrieus wind turbine is the rotor area which is represented by equation 3, where A is the total swept area, D is the rotor diameter, and H is the turbine height:

$$A = D \times H \quad [4]$$

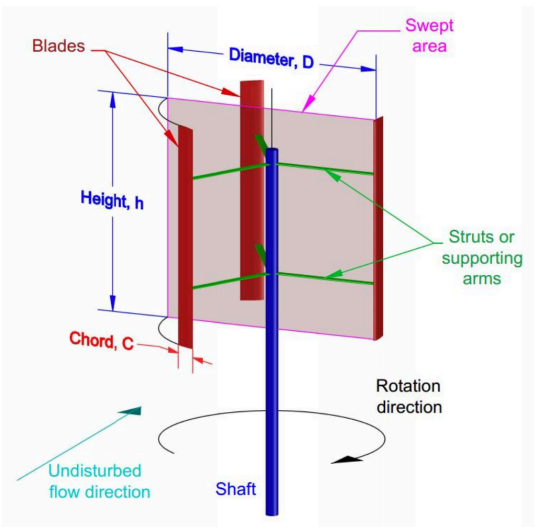

Figure 1.2 An illustration of a three-bladed VAWT. This clarifies the different components of the VAWT in addition to its main terminologies.

Figure 11. Diagram of Swept Area parameters for Darrieus wind turbines

The total electrical power output of the turbine is given by:

$$P_{output} = \mu \times P_{wind} \quad [5]$$

Where P_{output} is the real/usable power produced by the turbine (W), μ is the overall efficiency (dimensionless), P_{wind} and is the accessible wind power (W). Another important parameter in wind turbine calculations is the Tip Speed Ratio (TSR) also known as the Blade Speed Ratio (BSR). It is one of the most influential parameters in the design of Darrieus VAWTs and it represents the ratio between the tangential velocity of the blade and the undisturbed flow velocity, given by the equation below where ω is the rotational velocity in rad/s, R is the turbine radius and V is the undisturbed wind flow velocity:

$$TSR = \frac{\omega \cdot R}{V} \quad [6]$$

Velocity Triangles are another important aspect of wind turbine calculations. These are diagrams that illustrate how the absolute velocity of a fluid, the tangential velocity of a blade, and the relative velocity of the fluid interact within turbomachinery, such as pumps or turbines [43].

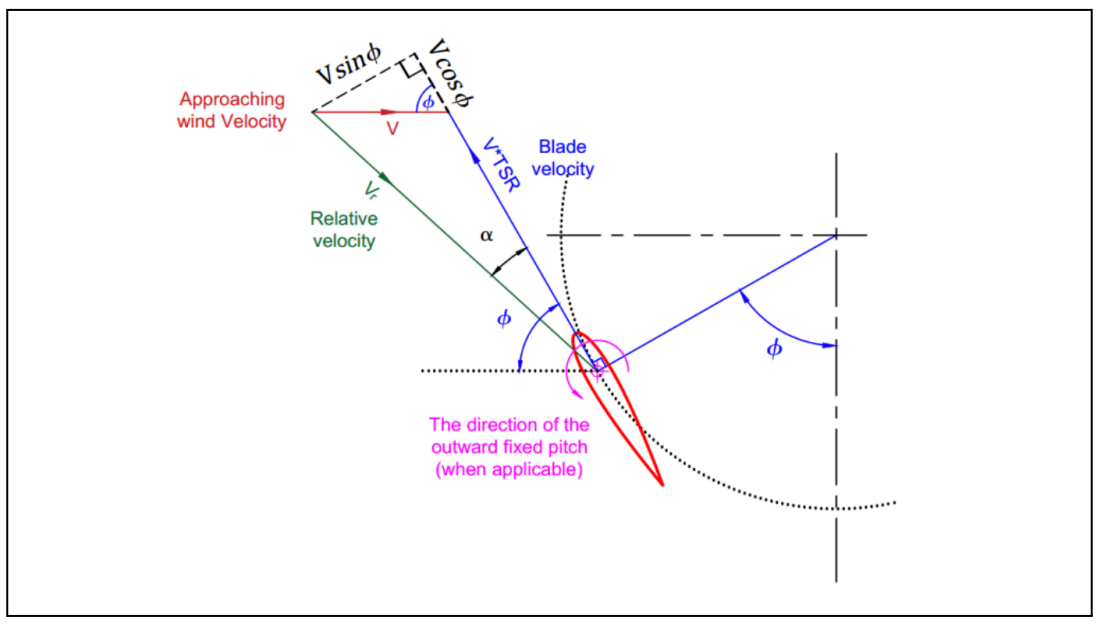

Figure 12. A velocity triangle schematic

Savonius Wind Turbines

Background:

Savonius turbines are the other main type of vertical axis wind turbine, designed and developed by a Finnish engineer named Sigurd Johannes Savonius [51]. Fig. 1 below shows two examples of Savonius wind turbines: one classical, and the other helical.

(a) (b)

Figure 13. (a) Classical Savonius type VAWT [54], (b) Helical style Savonius type VAWT [55].

Working principal:

A classical two-bladed Savonius wind turbine consists of two semicircular surfaces on opposite sides of a vertical shaft, one convex and the other concave as shown in Figure 13 [53][56]. Savonius turbines are drag based turbines, meaning the force responsible for their rotation is the

drag force [53]. The drag force is a force which acts in the opposite direction of the motion of any object moving with respect to the surrounding fluid. As the wind blows and comes into contact with the two opposite faced surfaces, lift and drag forces are exerted on them [58]. A greater drag force is exerted on the concave surface than the convex one. This difference in drag is what causes the rotation of the turbine [56]. This is why Savonius turbines are known as “drag-based” turbines. Since Savonius turbines operate on drag, they cannot rotate faster than the wind speed. This means that the Tip Speed Ratio (TSR) is always between 0 and 1 for Savonius turbines [53].

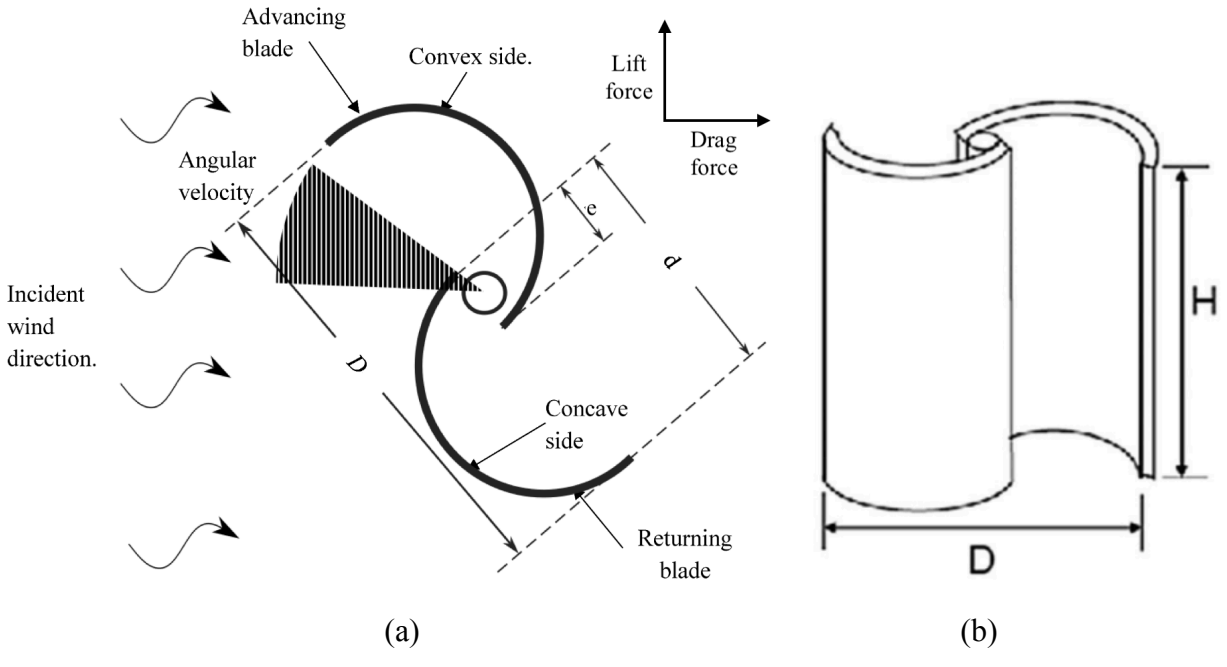

Figure 14. The Savonius wind turbine diagrams, (a) adapted from [56], (b) adapted from [57]

Benefits and Drawbacks:

Savonius wind turbines have many advantages including their simple construction and installation, low cost, ability to operate at slow wind speeds, self-starting capacity, and their independence of wind direction [53][56][57]. The low operating speed of Savonius wind turbines also make them lower noise when compared to other VAWTs. These qualities make them attractive for regions with high turbulence intensity and low wind speeds [56]. However, they also suffer from major drawbacks, the most significant being high negative torque generated

during operation and the associated loss of efficiency. Negative torque is the resistive force that opposes the turbine's rotation, caused by the drag force on the returning blade as the wind pushes on it. This negative torque forces the turbine to overcome an additional force to start or continue rotating [56].

Calculations:

To evaluate the performance of a Savonius wind turbine, its total power output and the coefficient of power (C_p) need to be calculated. The following equations are all adapted from [56]. This can we done starting with the drag force, expressed in Equation (1) as follows:

$$F_D = \frac{1}{2} C_D A \rho V^2 \quad (1)$$

where F_D is the drag force, C_D is the coefficient of drag, A is the blade surface area of a single blade, ρ is the density of the fluid, and V is the velocity of the blades relative to the wind. This can be re-written in terms of the wind speed, U and angular velocity of the blades. For a classical Savonius turbine with two blades, the total drag for is represented in Equation (2):

$$F_D = \frac{1}{2} C_D \rho (U - \Omega r)^2 (2A) = C_D \rho A (U - \Omega r)^2 \quad (2)$$

The coefficient of power, which is defined as the ratio of the turbine's output power to the total power available in the wind is expressed in Equation (3), where T is the torque generated and S is the swept area

$$C_P = \frac{P_T}{P_A} = \frac{T\Omega}{\frac{1}{2}\rho S U^3} \quad (3)$$

The torque is related to the drag force, F_D, as shown in Equation (4):

$$T = F_d r \quad (4)$$

$$T = C_D \rho A r (U - \Omega r)^2 \quad (5)$$

$$P_T = C_D \rho A r \Omega (U - \Omega r)^2 \quad (6)$$

This can be expressed in terms of the Tip Speed Ratio (TSR, λ), which is defined as the ratio between the turbine's blade tip to the wind speed:

$$\lambda = \frac{\Omega r}{U} \tag{7}$$

$$\Omega r = U\lambda \tag{8}$$

$$P_T = C_D \rho A U \lambda [U(1 - \lambda)]^2 \tag{9}$$

$$P_T = C_D \rho A U^3 \lambda (1 - \lambda)^2 \tag{10}$$

The coefficient of power can be expressed in terms of the Tip Speed Ratio as follows:

$$C_P = \frac{C_D \rho A U^3 \lambda (1-\lambda)^2}{\frac{1}{2}\rho S U^3} = \frac{2C_D A \lambda (1-\lambda)^2}{S} \tag{11}$$

Another important metric is the torque coefficient, C_m, which is a measure of the turbine's efficiency at converting mechanical energy into torque at a given wind speed [59]:

$$C_m = \frac{T}{\frac{1}{2}\rho S U^2 r} \tag{12) [8]}$$

$$C_m = \frac{C_D A (U-\Omega r)^2}{\frac{1}{2} S U^2} = \frac{2C_D A (U-\Omega r)^2}{S U^2} \tag{13}$$

It is related to the coefficient of power as follows:

$$C_P = C_m \lambda \tag{14) [6]}$$

The equations for the coefficient of power and the coefficients of torque can be differentiated with respect to λ to calculate the TSR that maximizes either the coefficient of power or the coefficient of torque.

Parameters:

There are many parameters of a Savonius turbine that impact its performance including the overlap ratio (OR), aspect ratio (AR), tip speed ratio (TSR), the number of blades (n), and the blade shape [57]. In this section, each parameter will be defined and relevant research will be summarized.

Aspect ratio (AR):

The aspect ratio is the ratio between the height of the turbine, H, and its diameter, D, as defined in Figure (2).

$$AR = \frac{H}{D} \tag{15}$$

Mahmoud et al [60] reviewed configuration at aspect ratios (α) of 0.5, 1.0, 2.0, 4.0, and 5.0 and observed that increasing the aspect ratio caused the power coefficient to increase, keeping other parameters constant. Another study done by Kamoji [61] shows that an aspect ratio of 0.7 produced the maximum power coefficient of 0.21. A good performance is recorded by keeping the aspect ratio between the range $1.5 - 2$. However, most existing rotors keep the aspect ratios closer to 1.0 or structural reasons [57].

Overlap ratio (OR):

The overlap ratio (OR) is the ratio between of the distance of overlap between the two blades, e, and the chord length of the blades, d, as defined in Figure (2).

$$OR = \frac{e}{d} \tag{15}$$

The amount of wind passing through the gap between the blades increases with an increase in the overlap of the blades. This leads to wind flowing through the concave side to the returning blade, producing more thrust. Tania et al. [63] studied compared overlap ratios of 0.15, 0.2, 0.25, and 0.30 for a classical Savonius turbine and found that for wind speeds smaller than 4.0m/s, 0.15 is

a suitable OR, whereas for wind speeds greater than 4.0m/s, an OR of 0.30 was more appropriate. The variation in performance was accounted for by the turbulent character of the wind at higher speeds. Alom et al [64] performed an 2-D unsteady simulation around the rotor for elliptical blades, testing OR between 0.0 and 0.30. It was found that the coefficient of power was maximized for OR = 0.15 [57]. According to Blackwell [65], the value of the optimal OR is within the range 0.1 - 0.15. J. Menet [66] found that the OR must be between 0.15 and 0.3 [53].While there is no widespread agreement on the optimal OR, based on these studies, it appears that the optimal OR lies between 0.1 and 0.3, with 0.15 being a frequently cited number.

Number of blades:

The efficiency of a Savonius rotor is affected by the number of blades. Within literature, rotors with two, three, and four blades have been studied. Saha et al. [67] conducted experiments using single, double, and triple stages of Savonius turbine rotors and found that the optimal number of blades was independent of the number of stages. Ali [68] concluded that a two-blade Savonius rotor produced more power than a three-bladed rotor under the same testing conditions [57].

Blade shape:

Figure (3) shown below shows four different blade shapes (semicircular, benesh, elliptical, modified bach) tested by Alom et al. [64] both numerically and experimentally [57]. The findings of this study are summarized in Table (1)

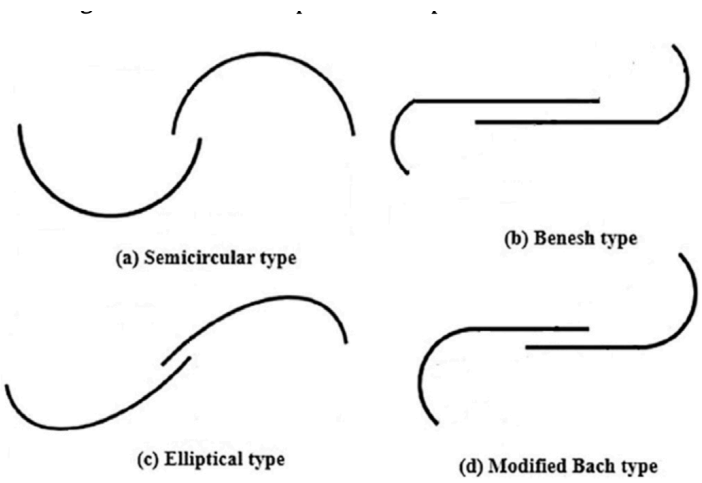

Figure 15. Savonius blade shapes [57]

Table 2: Results from Alom et al [64] study on the impact of blade shape on coefficient of power

Blade type	**Cp max numerical**	**Cp max wind tunnel**
Semi circular	0.272	0.158
benesh	0.294	0.159
Modified bach	0.304	0.162
elliptical	0.34	0.19

Lee et al. [67] examined the performance of helical-shaped Savonius wind turbines by varying the helical angle of the blades from 0° to 135°. A maximum power coefficient value was obtained at a blade twist angle of 45° [see Figure 4a]. There was a decrease in the power coefficient by 25.5% at a twist angle of 90° [57].

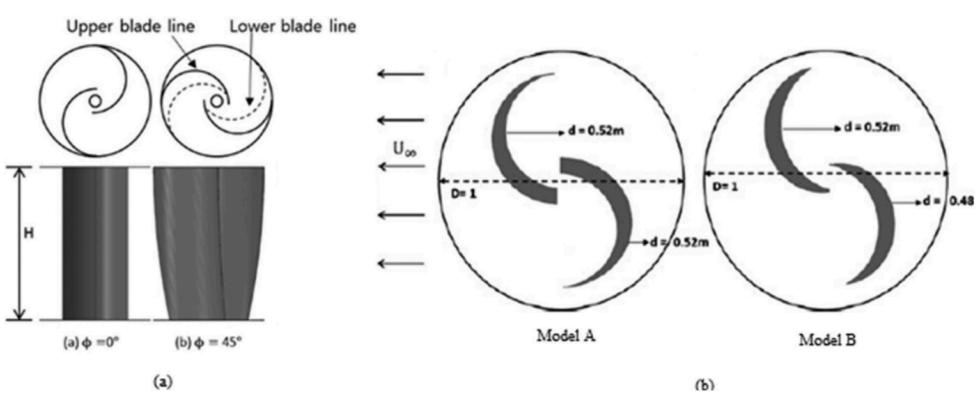

Figure 16: (a) Top and side views of blades with twist angle $\phi = 0°$ and $\phi = 135°$ [67] and (b) model A and model B [68][57].

Laws et al. [68] investigated two modified blade designs, Models A and B with respect to a conventional one and compared the power and torque generated using numerical methods [see Figure 4b]. Model-A showed a higher coefficient of power due to its reduced surface area at the blade tip and less pressure difference on both sides of the blade. Model-A and Model-B predicted

an improvement in coefficient of power over conventional blades of 28.12% and 10.53% respectively.

Many blade profile models other than the classical blade shape have been analyzed in terms of their performance. Altan et. al [69] compiled numerical and experimental studies from literature relating to blade shape which is summarized in Tables 2, 3, and 4 below.

Table 2: Power coefficients of Savonius wind turbines with and without interior design (i.d.) in terms of blade profile (blade shape) [69]

I.d. No	Reference	Study Type	Interior Design Name	C_p without i.d.	C_p with i.d.
1	Zhou and Rempfer [6]	Compared numerical	Bach-type	0.189	0.264
2	Kacprzak et al. [34]	Compared numerical	Bach-type	0.155	0.180
3	Kacprzak et al. [34]	Compared numerical	Elliptical blade	0.155	0.170
4	Mao and Tian [35]	Validated numerical	Blade arc angle	0.262	0.284
5	Alom and Saha [36]	Experimental Numerical	Vented elliptical blade	0.112	0.146
6	Alom and Saha [36]	Experimental Numerical	Non-vented elliptical blade	0.112	0.134
7	Ramadan et al. [37]	Experimental Numerical Genetic algorithm	S-shaped optimum blade design	0.140	0.280
8	El-Askary et al. [38]	Experimental Numerical	Twisted modified design	0.140	0.220
9	Damak et al. [39]	Experimental Numerical	Helical Bach design	0.180	0.200
10	Zemamou et al. [40]	Validated numerical Optimization Taguchi method	Bezier curved blade	0.270	0.350
11	Ramarajan and Jayavel [41]	Validated numerical	Three-fourth modified blade	0.230	0.250

Table 3: Power coefficients of Savonius wind turbines with and without interior design (i.d.) in terms of blade profile (blade attachment and blade surface geometry) [69]

I.d. No	Reference	Study Type	Interior Design Name	C_p without i.d.	C_p with i.d.
12	Sharma and Sharma [42]	Validated numerical	Multiple quarter blades	0.208	0.227
13	Deda Altan et al. [43]	Experimental Numerical	Additional design	0.099	0.119
14	Sharma and Sharma [44]	Validated numerical	Multiple miniature blades	0.192	0.213
15	Tian et al. [45]	Validated numerical Optimization	Optimal design	0.247	0.258
16	Ostos et al. [46]	Validated numerical	Two-quarters conventional blade	0.214	0.252
17	Haddad et al. [47]	Validated numerical	Additional inner blade	0.196	0.243
18	Gallo et al. [48]	Experimental Numerical	Multi-blade geometry	0.195	0.295
19	Al Absi et al. [49]	Experimental Numerical	Zigzag surface blade	0.260	0.292

Table 4: Power coefficients of Savonius wind turbines with and without interior design (i.d.) in terms of blade profile (different design and approach) [69]

I.d. No	Reference	Study Type	Interior Design Name	C_p without i.d.	C_p with i.d.
20	Roy and Saha [50]	Experimental Numerical	Newly developed blade	0.230	0.310
21	Tian et al. [51]	Validated numerical	Fullness of the blade	0.232	0.257
22	Roy and Ducoin [52]	Validated numerical	New blade design with moment arms	0.280	0.370
23	Zhang et al. [53]	Validated numerical Optimization	Optimal design	0.247	0.262
24	Chan et al. [54]	Numerical Genetic algorithm	Optimized blade	0.169	0.225
25	Marinic-Kragic et al. [55]	Validated numerical Optimization Genetic algorithm	Flexible-blade	0.220	0.238
26	Sobczak et al. [56]	Validated numerical	Deformable blade	0.210	0.400
27	Lajnef et al. [57]	Experimental Numerical	Novel delta-bladed	0.124	0.142
28	Imeni et al. [58]	Validated numerical	Airfoil-shaped blade	0.229	0.259

Augmentation devices to increase performance of Savonius wind turbines

To increase the efficiency and decrease the negative torque present in Savonius wind turbines, many augmentation devices, both internal and external, have been developed. These devices intend to direct wind to parts of the turbine and/or block it from sections.In the following section, a subsection of these devices will be explained.

Endplates:

Adding endplates to the top and bottom of the turbine prevents air from escaping from the tips of the concave side of the advancing and returning blades. The ratio of the diameter of the endplate, D_o to the diameter of the blades, D can be varied to maximize the coefficient of power [57].

Curtain arrangement:

A curtaining arrangement is made from wind deflecting plates that are placed in front of the rotor to direct the airflow [53].

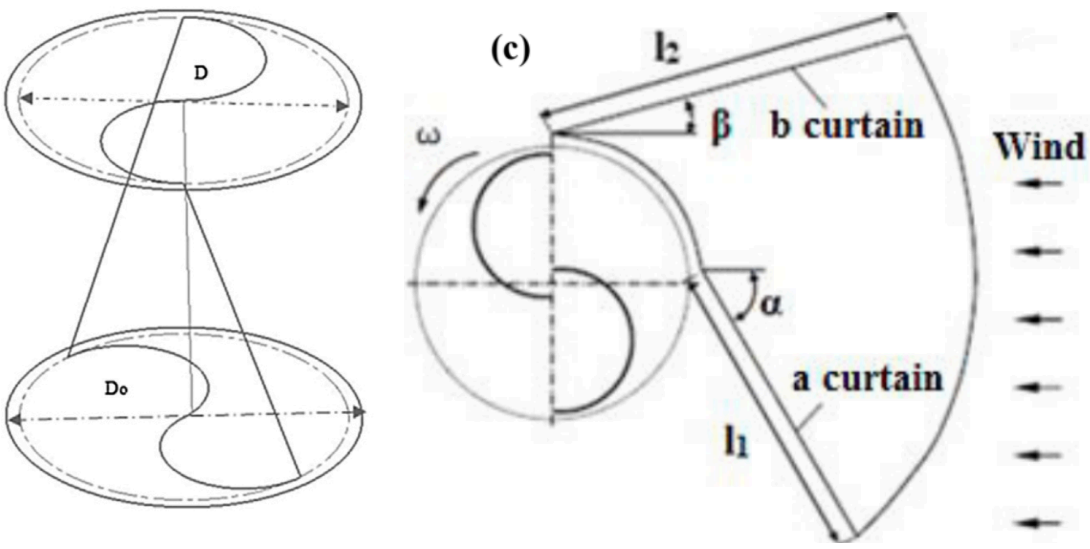

(a) (b)

Figure 17: (a) Circular end plate [57], (b) Curtaining arrangement [53]

Shielding obstacle:

Shielding obstacles are plates placed to shield the returning blades from this wind. Their purpose is to decrease negative torque and improve self-starting capabilities for the Savonius rotor [53][57].

Guide vanes:

Guiding vanes direct incoming wind toward the advancing blade and reduce air flow to the returning blade. They also provide a funneling effect, accelerating the wind in the upstream of the rotor [57].

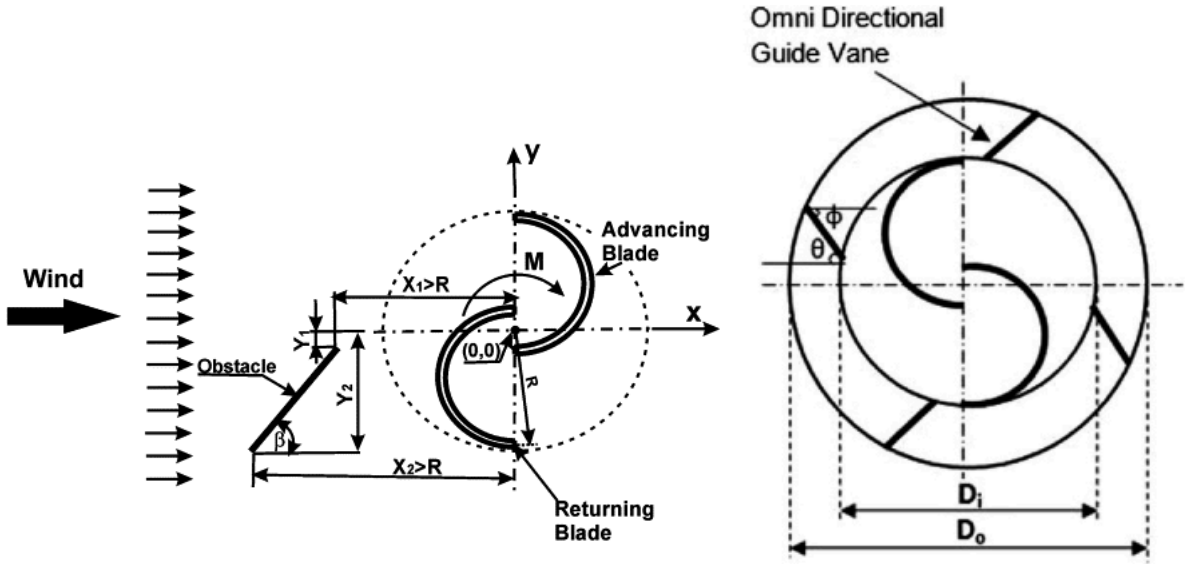

(a) (b)

Figure 18: (a) Shielding obstacle [69], (b) guiding vanes [70]

Miniature and quarter blades:

Miniature blades and quarter blades when placed concentrically within the rotor blades increase the efficiency of a Savonius wind turbine. The increased surface area leads to better utilization of the kinetic energy of the incoming wind [57]

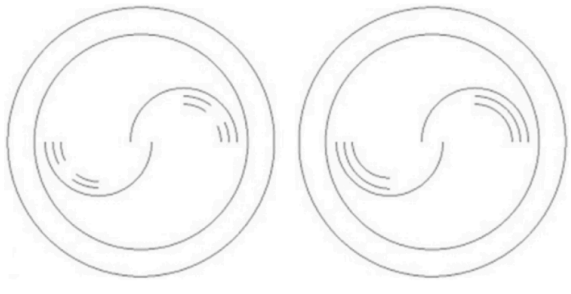

Figure 19: Multiple miniature and quarter blades [57]

An extensive compilation of both experimental and numerical studies of the impact of both interior and exterior designs on the coefficient of power are summarized in the following tables from [69].

Table 5: Power coefficient values of two-bladed Savonius wind turbines with and without exterior design (e.d.) [69]

(a)

E.d. No	Reference	Study Type	Exterior Design Name	C_p without e.d.	C_p with e.d.	Exterior Design
1	Irabu and Roy [4]	Experimental	Guide-box tunnel	0.225	0.276	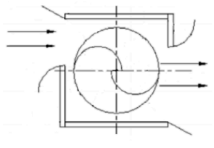
2	Deda Altan et al. [5]	Experimental	Curtain arrangement	0.160	0.380	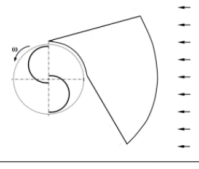
3	Mohamed et al. [19]	Validated numerical Optimization	Shielding obstacle	0.170	0.258	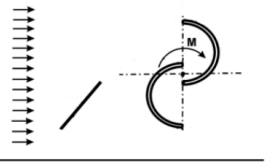

Table 1. *Cont.*

(a)						
E.d. No	**Reference**	**Study Type**	**Exterior Design Name**	**C_p without e.d.**	**C_p with e.d.**	**Exterior Design**
4	Tartuferi et al. [20]	Experimental Numerical	Conveyor-deflector curtain system	0.250	0.300	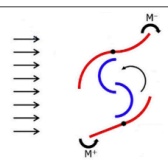
5	El-Askary et al. [21]	Validated numerical	Guide plates design	0.190	0.520	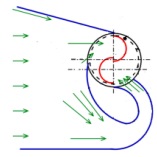
6	Kalluvila and Sreejith [22]	Experimental Numerical	Guide blade arrangement	0.180	0.280	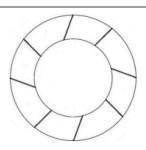
7	Mohammadi et al. [23]	Validated numerical	Nozzle design	0.130	0.363	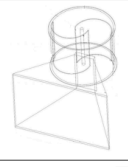
8	Layeghmand et al. [25]	Validated numerical	Airfoil-shaped deflector	0.237	0.313	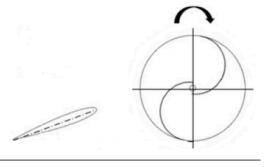

(b)						
E.d. No	**Reference**	**Study Type**	**Exterior Design Name**	**C_p without e.d.**	**C_p with e.d.**	**Exterior Design**
9	Yuwono et al. [26]	Experimental	Circular cylinder	0.178	0.200	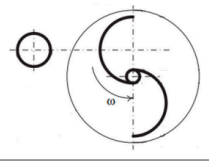
10	Nimvari et al. [27]	Validated numerical	Porous deflector	0.249	0.274	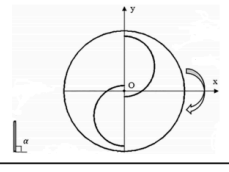

Table 1. *Cont.*

(b)						
E.d. No	**Reference**	**Study Type**	**Exterior Design Name**	**C_p without e.d.**	**C_p with e.d.**	**Exterior Design**
11	Yahya et al. [28]	Experimental	Guide vane	0.017	0.028	
12	Hesami et al. [24]	Validated numerical	Wind-lens	0.167	0.210	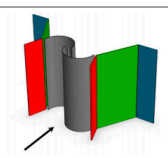
13	Hesami et al. [24]	Validated numerical	Wind-lens (with a dual turbine)	0.167	0.358	
14	Fatahian et al. [29]	Validated numerical	Nanofiber-based deflector	0.250	0.272	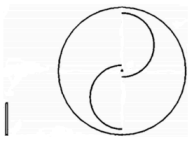
15	Marinic-Kragic et al. [30]	Validated numerical Optimization	Deflector blades	0.240	0.350	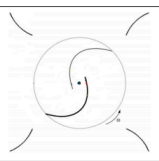
16	Tian et al. [31]	Validated numerical	Passive deflector	0.250	0.313	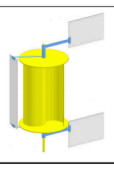

Table 6: Power coefficient values of three-bladed Savonius wind turbines with and without exterior design (e.d.) [69]

E.d. No	Reference	Study Type	Exterior Design Name	C_p without e.d.	C_p with e.d.	Exterior Design
1	Irabu and Roy [4]	Experimental	Guide-box tunnel	0.160	0.240	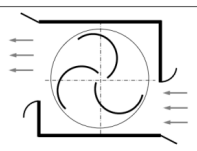
2	Mohamed et al. [19]	Validated numerical Optimization	Shielding obstacle	0.151	0.212	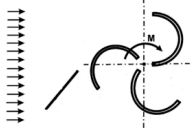
3	Yao et al. [32]	Numerical Experimental	Tower cowling	0.200	0.480	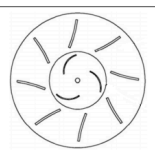
4	Manganhar et al. [33]	Experimental	Rotor house	0.125	0.218	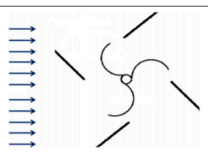

When the power coefficients of the design models in Tables 5 and 6 are compared, it can be seen that the two-bladed turbines generally have higher power coefficients than the three bladed turbines [69]. This is consistent with the findings of Ali [68], cited above.

Savonius summary

Savonius wind turbines are a drag-based VAWT technology that have a simple construction and installation, low cost, ability to operate at slow wind speeds, self-starting capacity, and their independence of wind direction. However, they struggle with low efficiency due to high negative torque. To address this, numerous augmentation devices have been developed to direct windflow toward the convex blade and away from the concave blade. While these strategies have been effective at increasing the coefficient of performance, they often increase the size and complexity of the turbine and reduce their effectiveness at receiving wind from all directions [69].

Structural Mechanics

A brief examination of the structural mechanics of the wind turbine towers was done. The overall loads on the Vertical Axis Wind Turbine towers can be divided into 3 main categories. These are the aerodynamic loads, wind loads on the tower, and the structural stress analysis [40]. Aerodynamic loads on a VAWT tower result from the cyclic lift forces on the rotating blades. The aerodynamic load calculations are based on two specific wind conditions: NWC (Normal Wind Conditions) and EWC (Extreme Wind Conditions). The maximum amount of thrust force that can be applied to a wind turbine is given by the design standards of small-size wind turbines and modeled below by equation 1:

$$F_{T_r} = \frac{1}{2} C_T \rho (2.5 \times V_{ave})^2 A \quad [1]$$

Where, F_{T_r} is the thrust force on the rotor measured in newtons, C_T is the thrust force coefficient which is equal to 0.5, A is the total swept area, and V is the average velocity of the wind. The wind loads on the tower can be calculated in a similar way, assuming wind is uniformly distributed, and this is modeled below in equation 2, where F_{T_t} is the thrust force on the tower, C_{T_t} is the coefficient of thrust force, V_{e50} is the extreme wind speed of 50 years (50-year-old extreme wind speeds ($Ve50$) and 1-year extreme wind speeds ($Ve1$) are used to calculate the maximum wind speeds that may occur in that period) [40].

:

$$F_{T_t} = \frac{1}{2} C_{T_t} \rho V_{e50}{}^2 A \quad [2]$$

There are also the gravitational loads which must be considered when analyzing the structural mechanics of VAWTs. These are the “dead loads” from the structure's weight including the tower, rotor, and other components. The overview of load distribution is modeled by figure 1 below:

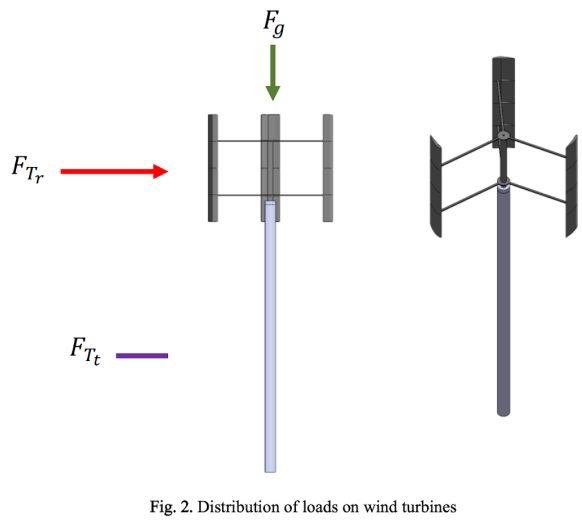

Fig. 2. Distribution of loads on wind turbines

Figure 20. The Distribution of loads on VAWTs

The structural stress analysis is given by equation 3 below, where F_g is the weight of the structure, A_b is the cross section of the tower, M is the flexural torque: internal torques generated within a structural member (like a beam) due to an external bending load, y is the distance from the neutral axis, and I is the moment of inertia.

$$\sigma_{max} = \frac{F_g}{A_b} \pm \frac{My}{I} \quad [3]$$

Conclusion

This memo provided a technical foundation for Darrieus and Savonius VAWT types, HAWTs vs VAWTs, and technical answers to some common questions. This memo did not aim to be a complete technical report on the design of VAWTs, and does not compile all of the information VAWT Ventures has on VAWTs, this information will be continuously worked on and gained throughout the design process. Additionally, some of the math/calculations sections of this memo will be further worked on. The augmentation topic for Savonius type VAWTs was not covered in detail, however will be researched further.

References

[1] A. L. Rødseth et al., “Evaluation of different turbine concepts for wind power,” *Academia.edu*, 2016. [Online]. Available: https://www.academia.edu/34918051/Evaluation_of_different_turbine_concepts_for_wind_power_pdf. [Accessed: Oct. 17, 2025].

[2] R. Neumann, J. Peinke, and G. M. H. Krauter, “Short-term power prediction of wind turbines based on stochastic analysis of wind measurements,” *J. Wind Eng. Ind. Aerodyn.*, vol. 175, pp. 61–68, 2018. doi: 10.1016/j.jweia.2018.01.003.

[3] A. S. Bahmani, E. Asgari, and H. Shafiee, “Vertical axis wind turbines: A review of recent developments,” *Renew. Sustain. Energy Rev.*, vol. 26, pp. 506–523, 2013. [Online]. Available: https://www.sciencedirect.com/science/article/abs/pii/S1364032113002116 . [Accessed: Oct. 17, 2025].

[4] E. Möllerström, F. Ottermo, J. Hylander, and H. Bernhoff, “Noise emission of a 200 kW vertical axis wind turbine,” *Energies*, vol. 9, no. 1, p. 19, 2016. doi: 10.3390/en9010019.

[5] A. Rosato, A. Perrotta, and L. Maffei, “Commercial small-scale horizontal and vertical wind turbines: A comprehensive review of geometry, materials, costs and performance,” *Energies*, vol. 17, no. 13, p. 3125, 2024. doi: 10.3390/en17133125.

[6] J. A. N. F. de Souza, P. P. N. de Souza, and C. A. P. Torres, “Techno-economic assessment of small vertical axis wind turbines for urban applications,” *Renew. Sustain. Energy Rev.*, vol. 91, pp. 26–42, 2018. doi: 10.1016/j.rser.2018.03.033.

[7] “How turbulence can impact wind power performance,” Wind Watch. [Online]. Available: https://www.wind-watch.org/documents/how-turbulence-can-impact-power-performance/. [Accessed: Oct. 17, 2025].

[8] “Frequently Asked Questions (FAQs): How much electricity does an American home use?” U.S. Energy Information Administration (EIA). [Online]. Available: https://www.eia.gov/tools/faqs/faq.php?id=427&t=3. [Accessed: Oct. 17, 2025].

[9] U.S. Energy Information Administration, “What is U.S. electricity generation by energy source?” [Online]. Available: https://www.eia.gov/tools/faqs/faq.php?id=427&t=3. [Accessed: Oct. 17, 2025].

[10] E. Möllerström, F. Ottermo, J. Hylander, and H. Bernhoff, “Evaluation of different turbine concepts for wind power,” Academia.edu, 2016. [Online]. Available: https://www.academia.edu/34918051/Evaluation_of_different_turbine_concepts_for_wind_power_pdf. [Accessed: Oct. 17, 2025].

[11] J. Luo, et al., “Life cycle assessment of wind turbines,” Sustainability, vol. 17, no. 9, p. 3859, 2023. doi: 10.3390/su17093859.

[12] S. S. Rao, “Vibration of structures with damping,” J. Sound Vib., vol. 305, no. 3-5, pp. 400-407, 2007. [Online]. Available: https://www.sciencedirect.com/science/article/abs/pii/S0378778807002939.

[13] G. Andrade, K. Boswijk, and A. Tonello, “Experimental study of vertical axis wind turbines,” Renew. Energy, vol. 56, pp. 1-9, 2013. [Online]. Available: https://www.sciencedirect.com/science/article/abs/pii/S0378778813006099.

[14] D. Lee, L. Tang, and B. Kim, “Wind power forecasting with machine learning models,” J. Wind Eng. Ind. Aerodyn., vol. 244, p. 105540, 2023. doi: 10.1016/j.jweia.2023.105540.

[15] S. Kumar and P. Sharma, “Techno-economic analysis of wind energy systems,” Renew. Sustain. Energy Rev., vol. 216, p. 114302, 2024. doi: 10.1016/j.rser.2024.114302.

[16] D. Larson, “Put windmills on utility poles,” Texas Monthly, 2024. [Online]. Available: https://www.texasmonthly.com/articles/put-windmills-on-utility-poles/. [Accessed: Oct. 17, 2025].

[17] M. Schmidt, “Energy harvesting in urban wind environments,” Energy Convers. Manag., vol. 48, no. 9, pp. 2711-2716, 2007. [Online]. Available: https://www.sciencedirect.com/science/article/abs/pii/S1471084606705455.

[18] “An urban wind farm is... tremendous potential,” BBC News, 2005. [Online]. Available: http://news.bbc.co.uk/2/hi/uk_news/england/manchester/4648371.stm. [Accessed: Oct. 17, 2025].

[19] U.S. Department of Energy, “Small wind guidebook – size considerations,” 2025. [Online]. Available: https://windexchange.energy.gov/small-wind-guidebook#size. [Accessed: Oct. 17, 2025].

[20] A. Khan, R. Abdel-Khalik, and S. Wang, “Optimization of a vertical axis wind turbine for maximum power extraction,” J. Renew. Sustain. Energy, vol. 9, no. 4, p. 043302, 2017. doi: 10.1063/1.4998730

[21] E. Möllerström, F. Ottermo, J. Hylander, and H. Bernhoff, Eigenfrequencies of a Vertical Axis Wind Turbine Tower Made of Laminated Wood and the Effect Upon Attaching Guy Wires, Licentiate Thesis, Halmstad University, Sweden, 2014. [Online]. Available: https://www.diva-portal.org/smash/get/diva2:782923/FULLTEXT01.pdf. [Accessed: Oct. 17, 2025].

[22] “How is sound measured?”, ProtectEAR, 2025. [Online]. Available: https://www.protectear.com/us/en/articles/post/how-is-sound-measured. [Accessed: Oct. 17, 2025].

[23] D. Bowdler and H. G. Leventhall, Wind Turbine Noise. Multi Science Publishing Company, Limited, 2011.

[24] E. Möllerström, F. Ottermo, J. Hylander, and H. Bernhoff, “Noise emission of a 200 kW vertical axis wind turbine,” Energies, vol. 9, no. 1, p. 19, 2016. doi: 10.3390/en9010019.

[25] M. Larsson et al., “Noise propagation from a vertical axis wind turbine,” in Proc. INTERNOISE2014, Melbourne, Australia, 2014. [Online]. Available: https://acoustics.asn.au/conference_proceedings/INTERNOISE2014/papers/p829.pdf. [Accessed: Oct. 17, 2025].

[26] A. Rosato, A. Perrotta, and L. Maffei, “Commercial small-scale horizontal and vertical wind turbines: A comprehensive review of geometry, materials, costs and performance,” Energies, vol. 17, no. 13, p. 3125, 2024. doi: 10.3390/en17133125.

[27] A. Smith et al., “Cost analysis of vertical axis vs. horizontal axis wind turbines,” Renew. Energy Reports, vol. 15, pp. 120-135, 2024. [Online]. Available: https://www.sciencedirect.com/science/article/pii/S2590174524001168. [Accessed: Oct. 17, 2025].

[28] “Turbine sound measurement,” Wind Measurement International. [Online]. Available: http://www.windmeasurementinternational.com/wind-turbines/turbine_sound-measurement.php. [Accessed: Oct. 17, 2025].

[29] Massachusetts Department of Environmental Protection, “Kingston Wind Independence Turbine Acoustical Study Final Technical Report,” August 2015. [Online]. Available: https://www.mass.gov/doc/august-2015-kingston-wind-independence-turbine-acoustical-study-final-technical-report-with/download. [Accessed: Oct. 17, 2025].

[30] “Why are vertical axis wind turbines not widely popular?”, Energy-Elege, 2025. [Online]. Available: https://energy-elege.com/why-are-vertical-axis-wind-turbines-not-widely-popular/. [Accessed: Oct. 17, 2025].

[31] “Vertical axis wind turbines,” CleanCurrent, 2025. [Online]. Available: https://www.cleancurrent.com/wind-energy/vertical-axis-wind-turbines/. [Accessed: Oct. 17, 2025].

[32] E. Möllerström, F. Ottermo, J. Hylander, and H. Bernhoff, "Evaluation of different turbine concepts for wind power," Academia.edu, 2016. [Online]. Available: https://www.academia.edu/34918051/Evaluation_of_different_turbine_concepts_for_wind_power_pdf . [Accessed: Oct. 17, 2025].

[33] A. De Wilde, W. Y. Szokolay, and E. J. de Kijzer, “Performance evaluation of urban wind turbines: The role of the built environment,” Buildings & Cities, vol. 4, no. 1, p. 491, 2023. DOI: 10.5334/bc.491. [Online]. Available: https://journal-buildingscities.org/articles/10.5334/bc.491. [Accessed: Oct. 17, 2025].

[34] M. Pasinelli, C. A. Kriticos, and S. R. Wilson, “Assessing the ecological impacts of wind farms on bird populations,” J. Appl. Ecol., vol. 59, no. 6, pp. 1185–1195, 2022. DOI: 10.1111/1365-2664.13853. [Online]. Available: https://besjournals.onlinelibrary.wiley.com/doi/full/10.1111/1365-2664.13853. [Accessed: Oct. 17, 2025].

[35] “Darrieus Wind Turbine Working,” Elprocus. [Online]. Available: https://www.elprocus.com/darrieus-wind-turbine-working/ . [Accessed: Oct. 17, 2025].

[36] S. Gunecha, “Exploring Wake Losses in Offshore Wind,” Empire Engineering. [Online]. Available: https://www.empireengineering.co.uk/exploring-wake-losses-in-offshore-wind/. [Accessed: Oct. 17, 2025].

[37] “Detailed Loss Factors,” Wind Energy - The Facts. [Online]. Available: https://www.wind-energy-the-facts.org/detailed-loss-factors.html. [Accessed: Oct. 17, 2025].

[38] “The Role of Darrieus vs. Savonius Designs in VAWT Efficiency,” Eureka. [Online]. Available: https://eureka.patsnap.com/article/the-role-of-darrieus-vs-savonius-designs-in-vawt-efficiency. [Accessed: Oct. 17, 2025].

[39] R. J. Barthelmie et al., “The effect of atmospheric stability on offshore wind farm wake losses,” Renewable Energy, vol. 70, pp. 58–70, 2014. [Online]. Available: https://www.sciencedirect.com/science/article/abs/pii/S096014811400603X. [Accessed: Oct. 17, 2025].

[40] M. K. Sharifi et al., “Wake effect on wind farm performance,” Energy Equipment and Systems, vol. 10, no. 3, pp. 235–248, 2022. [Online]. Available: https://www.energyequipsys.com/article_715681_7b5aaf15647c054c8c592b5b40a6eb06.pdf . [Accessed: Oct. 17, 2025].

[41] M. Elsakka, “Aerodynamic performance of vertical-axis wind turbines,” Ph.D. dissertation, Univ. of Sheffield, Sheffield, U.K., 2020. [Online]. Available: https://etheses.whiterose.ac.uk/id/eprint/27424/. [Accessed: Oct. 17, 2025].

[42] “Velocity Triangle,” KSB Centrifugal Pump Lexicon. [Online]. Available: https://www.ksb.com/en-global/centrifugal-pump-lexicon/article/velocity-triangle-1116038. [Accessed: Oct. 17, 2025].

[43] “Understanding the Aerodynamics of Wind Turbine Blades,” Turbit. [Online]. Available: https://www.turbit.com/post/understanding-the-aerodynamics-of-wind-turbine-blades. [Accessed: Oct. 17, 2025].

[44] “The Role of Darrieus vs. Savonius Designs in VAWT Efficiency,” Eureka Patsnap. [Online]. Available: https://eureka.patsnap.com/article/the-role-of-darrieus-vs-savonius-designs-in-vawt-efficiency. [Accessed: Oct. 17, 2025].

[45] “The Darrieus rotor usually suffers from a low starting torque,” Zenodo. [Online]. Available: https://zenodo.org/records/1108332. [Accessed: Oct. 17, 2025].

[46] J. Alam and M. T. Iqbal, “Design and development of hybrid vertical axis turbine,” in Proc. CCECE'09, St. John's, NL, 2009, pp. 178–183.

[47] I. Paraschivoiu, O. Trifu, and F. Saeed, “H-Darrieus wind turbine with blade pitch control,” International Journal of Rotating Machinery, vol. 2009, pp. 1–7, 2009.

[48] J. Decoste, A. Smith, D. White, D. Berkvens, and J. Crawford, “Self-starting Darrieus wind turbine,” Design Project Mech. 4020, Dalhousie University, Halifax, Canada, 2004.

[49] “Review of Vertical Wind Turbines,” PubMed Central (PMC). [Online]. Available: https://pmc.ncbi.nlm.nih.gov/articles/PMC8601092/. [Accessed: Oct. 17, 2025].

[50] D. Moyer, “Turbine Aerodynamics,” University of Chicago Department of Geophysical Sciences. [Online]. Available: https://geosci.uchicago.edu/~moyer/GEOS24705/Readings/turbine_aerodynamics.pdf. [Accessed: Oct. 17, 2025].

[51] L. Zhang, Y. Ge, H. H. L. Erickson, and S. K. P. Kumar, “Impact of intermittent renewable energy sources on power system stability,” Electr. Power Syst. Res., vol. 191, p. 106999, 2021. [Online]. Available: https://www.sciencedirect.com/science/article/abs/pii/S019689042031027X. [Accessed: Oct. 17, 2025].

[52] A. Yilmaz, S. K. Saha, and S. K. Dey, “Performance evaluation of wind turbines with different blade configurations,” Renewable Energy, vol. 155, pp. 1092–1104, 2020. [Online]. Available: https://www.sciencedirect.com/science/article/pii/S187661021735453X. [Accessed: Oct. 17, 2025].

[53] “Savonius wind turbine,” Netzero Guide. [Online]. Available: https://netzeroguide.com/savonius-wind-turbine/. [Accessed: Oct. 17, 2025].

[54] “LS-Helix 3.0,” Luvside. [Online]. Available: https://www.luvside.de/en/our-products/ls-helix-3-0/. [Accessed: Oct. 17, 2025].

[55] D. M. L. Schmidt, et al., “A review of wind turbine blade performance,” Energies, vol. 17, no. 15, p. 3708, 2024. [Online]. Available: https://www.mdpi.com/1996-1073/17/15/3708#B8-energies-17-03708. [Accessed: Oct. 17, 2025].

[56] S. M. A. Islam and M. K. Sarker, “Optimization of wind turbine components,” Energy Convers. Manag., vol. 236, p. 113942, 2021. [Online]. Available: https://www.sciencedirect.com/science/article/abs/pii/S2214785321037810. [Accessed: Oct. 17, 2025].

[57] R. K. Singh, et al., “Performance analysis of vertical axis wind turbines,” Energies, vol. 14, no. 7, p. 1962, 2021. [Online]. Available: https://www.mdpi.com/1996-1073/14/7/1962. [Accessed: Oct. 17, 2025].

[58] D. H. Ishraq and S. M. Sulaiman, “Design and building a rotor blade small wind turbine,” ResearchGate. [Online]. Available: https://www.researchgate.net/publication/320708396_Design_and_building_a_rotor_blade_small_wind_turbine_suitable_for_Iraq's_weather. [Accessed: Oct. 17, 2025].

[59] N. H. Mahmoud, A. A. El-Haroun, E. Wahba, and M. H. Nasef, “An experimental study on improvement of Savonius rotor performance,” Alex. Eng. J., vol. 51, no. 1, pp. 19–25, 2012.

[60] M. A. Kamoji, S. B. Kedare, and S. V. Prabhu, “Experimental investigations on single stage modified Savonius rotor,” Applied Energy, vol. 86, no. 7-8, pp. 1064–1073, 2009.

[61] R. Pudur and S. Gao, “Performance analysis of Savonius rotor on different aspect ratio for hydropower generation,” Proc.

[62] R. Tania, R. L. Florin, I. D. Adriana, M. Roxana, and A. Ancuta, “Experimental investigation on the influence of overlap ratio on Savonius turbines performance,” International Journal of Renewable Energy Research, vol. 8, pp. 1791–1799, 2018.

[63] A. Nur and U. Saha K., “Arriving at the optimum overlap ratio for an elliptical-bladed Savonius rotor,” in Proc. ASME Turbomachinery Tech. Conf. and Exposition, GT2017, ASME, 2017, pp. 1–10.

[64] B. F. Blackwell, “Wind tunnel performance data for two- and three-bucket Savonius rotors,” 1977.

[65] J. L. Menet and N. Bourabaa, “Increase in the Savonius rotors efficiency via a parametric investigation,” 2004.

[66] J.-H. Lee, Y.-T. Lee, and H.-C. Lim, “Effect of twist angle on the performance of Savonius wind turbine,” Renewable Energy, vol. 89, pp. 231–244, 2016.

[67] P. Laws, J. S. Saini, A. Kumar, and S. Mitra, “Improvement in Savonius wind turbine efficiency by modification of blade designs,” J. Energy Resour. Technol., vol. 142, pp. 1–12, 2020.

[68] “Performance of Savonius wind turbines,” MDPI, 2023. [Online]. Available: https://www.mdpi.com/2227-9717/11/5/1473. [Accessed: Oct. 17, 2025].

[69] M. A. Vaez and S. Movahedian, “Optimization of Savonius turbines,” Renew. Sustain. Energy Rev., vol. 14, no. 4, pp. 996–1005, 2010. [Online]. Available: https://www.sciencedirect.com/science/article/abs/pii/S0960148110001746. [Accessed: Oct. 17, 2025].

[70] Z. Zhang, et al., “Design and analysis of Savonius rotor with improved efficiency,” in Proceedings of the 10th International Conference on Renewable Energy and Sustainable Development, Springer, 2022, pp. 341–355. [Online]. Available: https://link.springer.com/chapter/10.1007/978-981-16-6738-1_24. [Accessed: Oct. 17, 2025].

[71] Lundquist, “How turbulence can impact power performance,” National Wind Watch, https://www.wind-watch.org/documents/how-turbulence-can-impact-power-performance/ (accessed Oct. 17, 2025).